A dihydrochalcone-specific O-methyltransferase from leaf buds of Populus trichocarpa implicated in bud resin formation

Eerik-Mikael Piirtola, Dawei Ma, Jürgen Ehlting & C. Peter Constabel

2025

Original citation:
Piirtola, E., Ma, D., Ehlting, J., & Constabel, C. P. (2025). A dihydrochalcone-specific O-methyltransferase from leaf buds of Populus trichocarpa implicated in bud resin formation. *Journal of Experimental Botany*, *76*(8), 2129–2143. https://doi.org/10.1093/jxb/eraf020

SOCIETY FOR EXPERIMENTAL BIOLOGY

Journal of Experimental Botany, Vol. 76, No. 8 pp. 2129–2143, 2025
https://doi.org/10.1093/jxb/eraf020 Advance Access Publication 22 January 2025

RESEARCH PAPER

A dihydrochalcone-specific *O*-methyltransferase from leaf buds of *Populus trichocarpa* implicated in bud resin formation

Eerik-Mikael Piirtola, Dawei Ma, Jürgen Ehlting, and C. Peter Constabel*

Centre for Forest Biology & Department of Biology, University of Victoria, 3800 Finnerty Road, Victoria, British Columbia, V8P 5C2 Canada

* Correspondence: cpc@uvic.ca

Received 28 March 2024; Editorial decision 14 January 2025; Accepted 21 January 2025

Editor: John Lunn, Max-Planck-Institute for Molecular Plant Physiology, Germany

Abstract

Production of secreted leaf bud resin is a mechanism for temperate trees to protect dormant leaf buds against frost damage, dehydration, and insect herbivory. Bud resins contain a wide variety of special metabolites including terpenoids, benzenoids, and phenolics. The leaf bud resins of *Populus trichocarpa* and *P. balsamifera* contain high concentrations of *O*-methylated dihydrochalcones, but the enzymes for methylating these compounds remain enigmatic. We used transcriptomics and differential gene expression analyses to identify a gene encoding a *P. trichocarpa* dihydrochalcone-specific *O*-methyltransferase, which we named PtDOMT1. Detailed enzymatic analyses demonstrated PtDOMT1 to be a highly selective and regiospecific *O*-methyltransferase which methylates 4 and 4′ positions of dihydrochalcones using *S*-adenosyl-L-methionine as a methyl donor. PtDOMT1 did not methylate any other flavonoid or phenolic substrate tested. These findings establish the final step in the biosynthesis of *O*-methylated dihydrochalcones in poplar and represent the first molecular analysis of leaf bud resin biosynthesis in plants.

Keywords: Dihydrochalcone, flavonoid, *O*-methyltransferase, phenylpropanoid, plant defense, poplar, resin.

Introduction

Temperate deciduous trees such as poplars and cottonwoods (*Populus* spp.) produce resistant leaf buds that protect the preformed leaves and remain dormant during the winter but flush out and develop in spring. The North American *P. trichocarpa* (black cottonwood) and *P. balsamifera* (balsam poplar) are known for their leaf buds covered with copious resin. This sticky exudate contains a variety of specialized metabolites and is thought to protect the leaf buds from frost during the winter and the developing leaves from insect herbivory during bud flush (Curtis and Lersten, 1974). Poplar bud resins are known to possess antimicrobial activities (Vardar-Ünlü *et al.*, 2008), and medicinal uses of poplar resin as ointments

Abbreviations: DHC, dihydrochalcone; 2′,4′,6′-OH DHC, 2′,4′,6′-trihydroxydihydrochalcone; 2′,4′,6′,4-OH DHC, phloretin, 2′,4′,6′,4-tetrahydroxydihydrochalcone; 2′,6′-OH-4′-OMe DHC, 2′,6′-dihydroxy-4′-methoxydihydrochalcone; 2′,6′,4-OH-4′-OMe DHC, asebogenin, 2′,6′,4-trihydroxy-4′-methoxydihydrochalcone; 2′,4′,6′-OH-4-OMe DHC, 2′,4′,6′-trihydroxy-4-methoxydihydrochalcone; 2′,6′-OH-4,4′-OMe DHC, 2′,6′-dihydroxy-4,4′-dimethoxydihydrochalcone, OMT, *O*-methyltransferase.

by North American First Nations are well documented (Moerman, 1998). Common traditional uses for preparations made from the resinous poplar bud exudate include wound treatment, dermatological and gastrointestinal aids, and as cold remedies.

Leaf bud resins from many poplar species including *P. nigra*, *P. trichocarpa*, *P. balsamifera*, and *P. tremuloides* have been characterized in detail by GC-MS and shown to contain diverse terpenoids, benzenoids, phenolic esters, flavonoids, and other phenylpropanoids (Greenaway *et al.*, 1989; English *et al.*, 1991, 1992; Kuś *et al.*, 2018). Notably, resins from closely related poplar species can have surprisingly distinct specialized metabolite profiles. Unlike foliar flavonoids which are typically glycosylated and accumulate in the vacuole, resin flavonoids accumulate as aglycones and are often secreted. Resin flavonoids may also contain one or more *O*-methylations (English *et al.*, 1991), which affects their solubility and contributes to the hydrophobic nature of the resin (Wollenweber and Dietz, 1981). Methylation of flavonoids also enhances antimicrobial activities and may be important for secretion or localization outside cells (Ibrahim *et al.*, 1987; Koirala *et al.*, 2016; Liu *et al.*, 2022). In *Populus deltoides*, the leaf bud resin is synthesized by secretory epidermal cells on the inner surface of bud scales and secreted during bud formation and maturation (Curtis and Lersten, 1974). *O*-Methylated flavonoid aglycones have been described in bud exudates of other trees including alders (*Alnus* spp.), birches (*Betula* spp.), hop-hornbeams (*Ostrya* spp.), horse chestnuts (*Aesculus* spp.), buckthorns (*Rhamnus* spp.), starburs (*Acanthospermum* spp.), cherries (*Prunus* spp.), and *Decarya madagascariensis* (Wollenweber and Dietz, 1981).

The bud resin chemical profiles of the closely related *P. trichocarpa* and *P. balsamifera* are characterized by an abundance of *O*-methylated dihydrochalcone aglycones, a subset of flavonoids structurally similar to chalcones but less widely distributed (Fig. 1) (Greenaway and Whatley, 1990; English *et al.*, 1991; Greenaway et al., 1992; Lavoie *et al.*, 2013). In *P. trichocarpa*, the methylated compounds 2′,6′-OH-4′-OMe dihydrochalcone (DHC) and 2′,4′,6′-OH-4-OMe DHC were reported as the most abundant representatives of this group (English *et al.*, 1991). *O*-Methylated dihydrochalcones are much less prevalent or absent in most other poplar species, but have been previously described in extracts of other plants such as *Piper aduncum* and *P. dennisii* (Orjala *et al.*, 1994; Cabanillas *et al.*, 2012). *O*-Methylated dihydrochalcones are known to be bioactive and may have therapeutic potential (Rivière, 2016). For example, dihydrochalcones as found in *P. trichocarpa* resin were shown to promote apoptosis in prostate cancer cells and could play a role in chemoprevention of cancer (Szliszka *et al.*, 2010). Dihydrochalcones can also have anti-tyrosinase activity, which suggests potential for treating hyperpigmentation, a skin condition caused by patchy overproduction of melanin (Mapunya *et al.*, 2011). Despite their presence in diverse plant families and their bioactive properties, the biosynthesis of *O*-methylated dihydrochalcones is not well understood (Ibdah et al., 2018), in particular how dihydrochalcones are methylated.

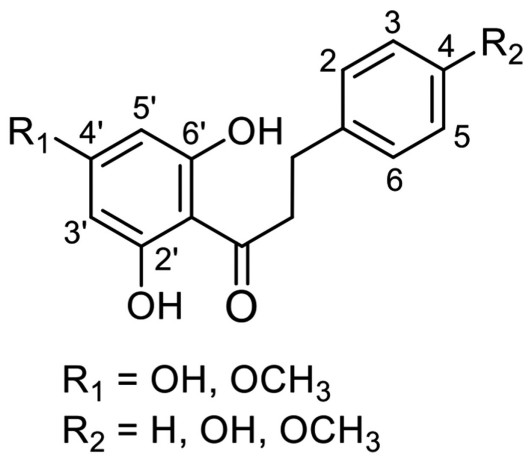

Fig. 1. General structure and substitution pattern of dihydrochalcones in *Populus trichocarpa* and *Populus balsamifera* leaf bud resin.

O-Methyltransferases (OMTs) in plants contribute to the diversity of specialized plant metabolites by methylating hydroxyl groups of phenolics, terpenoids, alkaloids, or other metabolites (Lam *et al.*, 2007; Barakat *et al.*, 2011; Lashley *et al.*, 2023). Flavonoid OMTs represent the largest group among known OMT enzymes, and these generally fall into the group of non-cation-requiring class II OMTs (Ibrahim et al., 1998). By contrast, the cation-requiring class I OMTs include enzymes such as caffeic acid OMT involved in methylation of lignin precursors (Vanholme *et al.*, 2010; Lashley *et al.*, 2023). However, both types of OMTs can be involved in flavonoid methylation, in some cases methylating the same compound but at different positions (Cui *et al.*, 2022). Flavonoid OMTs have been characterized in detail from many plant species (Kim *et al.*, 2010) including sweet basil (*Ocimum basilicum*) (Berim *et al.*, 2012), wild tomato (*Solanum habrochaites*) (Schmidt *et al.*, 2011, 2012), and peach (*Prunus percia*) (Cheng *et al.*, 2014). They can be regioselective and have been shown to produce distinct substitution patterns on flavonoid substrates (Berim *et al.*, 2012; Liu *et al.*, 2022). While some OMTs are highly selective for a single position on a narrow range of substrates, others produce multiple methylations on a broad spectrum of flavonoid substrates (Berim *et al.*, 2012; Berim and Gang, 2016; Lashley *et al.*, 2023). The only characterized OMT reported from poplar to date is a *P. deltoides* flavone 7-OMT, which is specifically methylates at the 7 position and has a strong preference for flavones and flavonols (Kim *et al.*, 2006).

OMTs that act on dihydrochalcones have not been previously characterized in any plant species. Here, we use chemical analysis, transcriptomics, phylogenetic gene family reconstruction, and enzyme assays to identify a novel OMT that specifically methylates dihydrochalcones in leaf bud resin of *P. trichocarpa*. Our data indicate that this enzyme is responsible for the seasonal accumulation of methylated dihydrochalcones in the resins of these species, providing

new opportunities for the molecular analysis of bud resin biosynthesis.

Materials and methods

Sampling of *P. trichocarpa* and *P. balsamifera* lateral leaf buds

Poplar leaf bud samples of *P. trichocarpa* (Nisqually-1) were collected from 15-year-old trees on the University of Victoria's Forest Biology Research Compound (48°27′N, −123°18′W). Lateral leaf buds of *P. trichocarpa* were collected monthly over 1 year to examine seasonal patterns of *PtDOMT1* expression. For each sampling, 10 leaf buds were collected from three adjacent clonal trees, which acted as biological replicates. Three replicate sample sets were gathered from each of the biological replicates. To study differences in the accumulation of dihydrochalcones and expression of PtDOMT1 in different leaf bud tissues, leaf bud scales and the enclosed embryonic leaf tissues were manually separated from samples collected from April to August.

To examine leaf bud development and leaf bud resin accumulation in a more controlled setting, dormant cuttings of female *P. trichocarpa* (Nisqually-1) and female *P. balsamifera* (LOV-5) were induced to flush in a growth chamber. Dormant cuttings of *P. balsamifera* were acquired from Dr Raju Soolanayakanahally (Agriculture and Agri-Food Canada, AAFC) in Saskatoon, Canada. The dormant poplar cuttings, harvested in February, were ~30 cm long and were stored at 4 °C in the dark until use. To induce bud break, dormant twigs were placed in water in a growth chamber at 22 °C under 16 h of light and sampled at 2 d intervals. For each time point, leaf buds were collected from one individual cutting as a replicate to prevent wound-induced effects during the time course. Samples were collected from three replicates of *P. balsamifera* and two replicates of *P. trichocarpa*. Each sampling consisted of 10 leaf buds, and samples were collected over 12 d (Supplementary Fig. S1). All samples were frozen immediately in liquid nitrogen, ground in liquid nitrogen, and stored at −80 °C prior to extraction.

Targeted metabolite analysis by UPLC-MS

Metabolites from whole leaf buds were extracted from accurately weighed frozen ground poplar leaf buds (40 mg) with 1 ml of methanol. The samples were vortexed, sonicated for 10 min in a sonicating water bath, and centrifuged for 10 min at 21 000 *g* to pellet the plant material. The supernatant was collected, and the pellet re-extracted with 1 ml of methanol using the same procedure. Both extractions were combined, and the pooled extracts were dried in an Eppendorf SpeedVac concentrator. The dried extracts were stored at −20 °C until the analysis. For quantification of dihydrochalcones, the whole leaf bud extracts were reconstituted in 1 ml of methanol, and diluted 10 times with methanol before analysis. The samples were analyzed using a Waters Acquity UPLC System coupled with an Acquity PDA eLambda Detector and an Acquity QDa single quadrupole mass spectrometer (Waters, Milford, MA, USA). The column used for separation was a Waters BEH C_{18} (50 mm×2.1 mm ID, 1.7 µm). The column temperature was set to 40 °C, and the autosampler temperature was 10 °C. The two-solvent gradient consisted of solvent A [ddH_2O with 0.1% formic acid (v/v)] and solvent B [acetonitrile with 0.1% formic acid (v/v)] at a flow rate of 0.5 ml min^{-1}. The gradient was as follows: 0.1% B (0–0.5 min), 0.1–50% B (0.5–5 min), 50–90% B (5–8 min), 90% B column wash (8–9 min), 90–0.1% B (9–9.1 min), and 0.1% B for column equilibration (9.1–11 min). The UV detector range was 190–800 nm. The MS conditions were as follows: capillary voltage 0.8 kV, probe temperature 600 °C, source temperature 150 °C, and cone gas (N_2) flow. The MS full scan range was 50–1000 *m/z*, and the MS analysis was performed using the negative ionization mode.

The compound-specific MS data were collected using selected ion recording (SIR) methods optimized for the predominant molecular ion $[M-H]^-$ of each compound of interest. The optimized SIR methods were as follows: phloretin (2′,4′,6′,4-OH DHC, 273 *m/z*, 15 V), asebogenin (2′,6′,4-OH-4′-OMe DHC, 287 *m/z*, 15 V), 2′,4′,6′-trihydroxydihydrochalcone (2′,4′,6′-OH DHC, 257 *m/z*, 15 V), 2′,6′-dihydroxy-4′-methoxydihydrochalcone (2′,6′-OH-4′-OMe DHC, 271 *m/z*, 15V), 2′,6′-dihydroxy-4,4′-dimethoxydihydrochalcone (2′,6′-OH-4,4′-OMe DHC, 301 *m/z*, 15 V), and 2′,4′,6′-trihydroxy-4-methoxydihydrochalcone (2′,4′,6′-OH-4-OMe, 285 *m/z*, 15 V). Calibration curves for each compound were prepared by using a concentration range of 0.05–100 µg ml^{-1}. MS data were processed and the peak areas were integrated using TargetLynx (Version 4.2). Samples were normalized by the fresh weight of the extracted whole buds. Analytical standards for 2′,4′,6′-OH DHC, 2′,4′,6′-OH-4-OMe DHC, and 2′,6′-OH-4,4′-OMe DHC were acquired from Biosynth Carbosynth (San Diego, CA, USA) and 2′,4′,6′,4-OH DHC, 2′,6′,4-OH-4′-OMe DHC, and 2′,6′-OH-4′-OMe DHC were acquired from TransMIT (Giessen, Germany).

RNA extraction and quantitative reverse transcription–PCR analysis

Total RNA was extracted from the lateral leaf buds as described by Muoki *et al.* (2012). Extracted RNA was treated with RQ1 DNase (Promega, Madison, WI, USA) to remove genomic DNA, and the ProtoScript® II Reverse Transcriptase kit (New England Biolabs, Whitby, ON, Canada) was used for first-strand cDNA synthesis. Quantitative reverse transcription–PCR (RT–qPCR) analysis was performed using Luna® Universal qPCR Master Mix (New England Biolabs, Whitby, ON, Canada) in a total volume of 15 µl employing a protocol adapted and scaled down from the manufacturer. Each reaction contained 1 µl of 1:10 diluted cDNA template. PtDOMT1 transcript abundance was measured using forward primer 5′-ATGTTGTAGCAACAGCACCA-3′ and reverse primer 5′-TCATCGGTCCAATCATGCAA-3′ (Supplementary Table S1). Primer annealing efficiency was optimized using a dilution series of cDNA templates prior to quantitative analysis. The primer efficiency of PtDOMT1 was 95.75% (R^2=0.9936) at 58 °C, yielding a 121 bp amplicon. PtDOMT1 transcript abundance was normalized using the geometric mean of ubiquitin (UBQ10; Potri.014G115100) and actin (ACT; Potri.001G309500) as housekeeping genes. Samples without cDNA templates were used as negative controls.

RNA-seq analysis

Total RNA was purified from lateral leaf buds of *P. trichocarpa* and *P. balsamifera* cuttings induced to flush as described above. Samples collected at day 0 (D_0), day 4 (D_4), and day 10 (D_{10}) were selected to represent dormant, pre-bud break, and bud break phases of the lateral leaf buds, respectively. Three biological replicates of *P. balsamifera* and two biological replicates of *P. trichocarpa* were used to prepare RNA-seq libraries as previously described using the NEBNext® Ultra™ RNA Library Prep Kit for Illumina® (New England Biolabs) (Ma *et al.*, 2018). A total of 15 RNA libraries were pooled together and sequenced on one HiSeq lane using the Illumina NextSeq 550 platform by the University of British Columbia Sequencing and Bioinformatics Consortium (Vancouver, BC, Canada).

Sequence alignment of the raw RNA-seq data was performed using HiSAT2 (Kim et al., 2019), and Cufflinks (Trapnell et al., 2012) was used for transcript assembly. The *P. trichocarpa* v4.1 genome was used as a reference genome sequence (Goodstein *et al.*, 2012; http://phytozome.jgi.doe.gov). Differential expression analysis to compare gene expression patterns at 4 d and 10 d after bud flush induction relative to day 0 was conducted using the DESeq2 package (Love *et al.*, 2014) in R (version

4.3.1). The annotated *P. trichocarpa* v4.1 reference transcriptome (http://phytozome.jgi.doe.gov) was used for gene functional annotation.

Phylogenetic analysis

Amino acid sequences for phylogenetic analysis of plant OMTs were downloaded from the National Centre for Biotechnology Information (NCBI) (https://www.ncbi.nlm.nih.gov/protein/) with accession numbers as listed below. Multiple sequence alignments were performed in Mega11 (v 11.0.13) using the ClustalW algorithm. Phylogenetic analysis was performed using the maximum-likelihood statistical method and the Jones–Taylor–Thorton (JTT) model with 1000 bootstrapping replicates. The graphical presentation of the phylogenetic tree was generated using FigTree (v 1.4). Names, accession numbers, and plant species of OMTs used in the phylogenetic analysis were as follows: ShMOMT1 (ADZ76433, *S. habrochaites*), ShMOMT2 (ADZ76434, *S. habrochaites*), ShMOMT3 (AGK26768, *S. habrochaites*), ObEOMT1 (Q93WU2, *O. basilicum*), ObCVOMT1 (Q93WU3, *O. basilicum*), CrOMT2 (Q8GSN1, *Catharanthus roseus*), PkHOMT1 (Q43046, *P. sieboldii*×*P. grandidentata*), ObFOMT1 (AFU50295, *O. basilicum*), ObFOMT2 (AFU50296, *O. basilicum*), ObFOMT3 (AFU50297, *O. basilicum*), ObFOMT4 (AFU50298, *O. basilicum*), ObFOMT5 (AFU50299, *O. basilicum*), ObFOMT6 (AFU50300, *O. basilicum*), MsIOMT8 (O24529, *Medicago sativa*), MsIOMT6 (O22308, *M. sativa*), MsIOMT9 (O22309, *M. sativa*), MsCOMT (AAB46623, *M. sativa*), SlAOMT (NP_001289828, *Solanum lycopersicon*), HlOMT1 (ABZ89565, *Humulus lupulus*), HlOMT2 (B0ZB56, *H. lupulus*), MsOMT (AAB48059, *M. sativa*), and NtCOMT2 (AAL91506, *Nicotiana tobacum*). The sequence for PdOMT7 (TC29789, *P. deltoides*) is not present in the NCBI databases, but was obtained from Dr Anna Berim, Washington State University.

Recombinant protein expression and purification

The coding sequences of candidate genes were synthesized by Twist Bioscience (South San Francisco, CA, USA). The vector construct included the N-terminal His-tagged expression vector pET-28a(+), containing *Xho*I and BamHI restriction sites and *Escherichia coli* codon-optimized insert sequences. The recombinant vector was transferred into electrocompetent *E. coli* (BL21 DE3) via electroporation, and the transformed colonies were selected on LB plates containing 50 μg ml^{-1} kanamycin after incubation overnight at 37 °C. A single colony was transferred into a liquid starter culture containing 6 ml of LB medium and 50 μg ml^{-1} kanamycin. For protein induction, 4 ml of the liquid culture was transferred into 100 ml of fresh LB medium and incubated at 37 °C and 250 rpm. After the liquid culture OD_{600} reached 0.4–0.6, isopropyl- β-D-thioglactopyranoside (IPTG) was added to the induction culture to a final concentration of 1 mM. The induction culture was incubated for 24 h at 20 °C and 250 rpm, after which the culture was centrifuged at 3220 x *g* and 4 °C for 20 min to harvest the cells. The supernatant was discarded, and the cell pellet was used for protein purification. The recombinant proteins were purified using Ni–NTA agarose (Qiagen, Hilden, Germany) employing the manufacturer's protocol. Protein fractions were pooled and desalted using centrifugal concentrator columns (30 kDa, Sigma-Aldrich) and exchange buffer (50 mM Tris–HCl, 10% glycerol, 1 mM DTT, pH 7.5). The concentration of the purified protein was determined using the Pierce™ BCA Protein Assay kit (ThermoFisher) against a BSA standard curve.

The purity and molecular weight of the recombinant proteins were confirmed by electrophoresis using standard methods. A 1 μg sample of the purified protein was separated using SDS–PAGE on a 12% acrylamide mini gel. Coomassie staining was used to confirm the molecular size of the purified product, and western blot was used to confirm the presence of the His-tagged protein. A 0.2 μm polyvinylidene difluoride (PVDF) membrane (Bio-Rad) was used for western blotting. The membrane was blocked for 1 h with 3% BSA/Tris-buffered saline (TTBS) and then incubated for 1 h with a His-tag mouse monoclonal antibody (1:5000; Cell Signaling Technology). After three washes with TTBS, the His-tagged recombinant proteins were visualized using a DAB (3,3′-diaminobenzidine) substrate kit (Bio Basic, Markham, ON, Canada).

Enzyme assays

Standard OMT assays consisted of a reaction mixture containing 5 μg of purified recombinant protein, 100 μM of the acceptor substrate, 500 μM *S*-adenosyl-L-methionine (SAM) (Sigma-Aldrich), and 1 mM DTT in 0.1 M sodium phosphate buffer (pH 7.5) in a total reaction volume of 200 μl. The reactions were incubated for 20 min at 30 °C and stopped with 20 μl of 6 N HCl. Samples were then centrifuged for 5 min at 15 000 rpm at 4 °C and the resulting supernatant was used directly for UPLC-MS analysis. Controls for the enzyme activity assays included boiled enzyme preparations as negative controls and previously characterized flavonoid OMT recombinant proteins from sweet basil (*O. basilicum*), ObFOMT1, ObFOMT3, and ObFOMT5 as positive controls (Berim *et al.*, 2012). Reaction linearity was tested by measuring the reaction product at 5 min intervals for 30 min at pH 7.5 and 30 °C.

To determine the pH optimum of the enzyme reactions, a pH range from 3 to 10 was covered using 0.1 M citrate-phosphate buffer (for pH 3–5), 0.1 M sodium phosphate buffer (for pH 6–8), and 0.1 M glycine-NaOH buffer (for pH 8.6–10). The optimal pH was determined by measuring the product concentration after 20 min incubation at 30 °C. Reaction temperature was tested at 5 °C intervals in the 10–50 °C range at pH 7.5 after 20 min incubation. The substrate for reaction condition optimization was 2′,4′,6′-OH DHC. The reaction buffer was preconditioned at tested temperatures for 10 min prior to the addition of the recombinant protein.

The kinetic properties for each substrate were determined at pH 7.5 and 30 °C with saturating concentrations of the methyl donor and varying concentrations of the methyl acceptor (5–300 μM). All kinetic parameters were measured in three replicates using independent recombinant protein preparations. The reaction products were analyzed by UPLC-MS using optimized SIR methods, as mentioned above, and the peak areas were used to determine the product concentration employing standard curves. The product concentration was used to calculate Michaelis–Menten kinetic parameters employing non-linear regression analysis in GraphPad Prism (Version 8.4.3).

Statistical analysis

Statistical analysis of the chemical data was performed using two-way ANOVA and Tukey's honestly significant difference (HSD) test employing GraphPad Prism (Version 8.4.3). Pairwise comparisons of relative gene expression were performed by paired *t*-tests. The Michaelis–Menten kinetic parameters were calculated using non-linear regression analysis.

Results

Dihydrochalcone composition of *P. trichocarpa* and *P. balsamifera* lateral leaf buds

We used targeted UPLC-MS methods to characterize the chemical diversity of dihydrochalcones in the leaf buds of *P. trichocarpa* and *P. balsamifera*. Dormant lateral leaf buds on short twigs were induced to flush for 4 d in a growth chamber, and whole buds were harvested and extracted. The concentrations of the major dihydrochalcones were higher in *P. balsamifera* leaf

buds compared with *P. trichocarpa* (Fig. 2A; Supplementary Figs S2, S3), with the exception of the non-methylated 2′,4′,6′,4-OH DHC which showed no significant difference. This compound was found at the lowest concentration in both species. However, the other non-methylated dihydrochalcone, 2′,4′,6′-OH DHC, was present at concentrations comparable with the methylated compounds. Overall, the resin of both species contained significant concentrations of singly and doubly methylated dihydrochalcones, with methyl groups on either the 4 or 4′ positions but not on any other available hydroxyl group. The *P. balsamifera* resin was characterized by high 2′,6′-OH-4′-OMe DHC and 2′,4′,6′-OH-4-OMe DHC content, while *P. trichocarpa* resin showed a more even distribution of the measured compounds, but contained proportionally little 2′,6′-OH-4′,4-OMe DHC compared with *P. balsamifera*.

In addition to the whole leaf bud extracts, the abundance of dihydrochalcones was assayed separately in bud scales and leaf tissue of *P. trichocarpa* leaf buds that were collected from developing lateral buds on young trees. Leaf bud scales were separated from embryonic leaf tissues of dissected leaf buds harvested in April (during bud break) and in August (young intact leaf buds). On a fresh weight basis, in April leaf tissue samples had a nearly 2-fold higher dihydrochalcone concentration than the bud scales (Fig. 2B). This difference was less pronounced for August samples (Fig. 2C). Overall, both leaf bud tissues contained substantially higher concentrations of dihydrochalcones in August compared with April.

Transcriptomic analysis and identification of candidate genes in *P. trichocarpa* and *P. balsamifera* lateral leaf buds

In order to identify candidate genes encoding dihydrochalcone-specific OMTs, we generated RNA-seq transcriptomes for *P. trichocarpa* and *P. balsamifera* leaf buds. A total of 33 582 and 33 404 unique transcripts were identified and annotated for *P. trichocarpa* and *P. balsamifera*, respectively. Based on gene annotation using the *P. trichocarpa* genome (version 4.1), a total of 36 OMTs were expressed in the leaf bud samples across both species. Thirteen OMTs uniquely expressed in *P. trichocarpa* and 14 OMTs in *P. balsamifera* (Supplementary Table S2) were identified, including nine candidate OMTs expressed in both. Phylogenetic analysis of the nine common candidate genes together with previously characterized OMTs (Fig. 3) suggested possible substrate classes for the candidate genes. In this phylogeny, Potri.013G136300, Potri.013G143800, and Potri.019G102900 were within a clade containing HlOMT2, an OMT which has been shown to act on the 4′ position of chalcones, making these the strongest candidates for encoding OMTs relevant to methoxylated dihydrochalcones found in poplar. A comparison of the Potri.013G136300 and Potri.013G143800 peptide sequences indicated that these two genes shared 99.4% similarity and are likely to be recently duplicated paralogs. Potri.013G136300 was selected to represent this paralog pair for further analysis since it showed greater expression in both poplar species. HlOMT1 alignment with Potri.019G102900 displayed 56.29% similarity. Alignment of HlOMT2 with Potri.013G136300 and Potri.019G102900 showed 51.97% and 57.1% similarity, respectively. We also obtained the nucleotide sequence of a previously studied *P. deltoides* OMT gene, *PtOMT7*, which proved to be very similar to Potri.013G136300. The *PtOMT7* gene product was demonstrated to have methyltransferase activity with both flavonols and flavones, but assays with chalcones or dihydrochalcones were not reported (Kim *et al.*, 2006).

To gain further insight into the putative candidate OMT genes, we looked for co-expression patterns within both *P. trichocarpa* and *P. balsamifera* datasets. We reasoned that relevant OMTs should be up-regulated during bud break in parallel with core phenylpropanoid and flavonoid pathway genes such as phenylalanine ammonia-lyase (*PAL*) and chalcone synthase (*CHS*) that act upstream of dihydrochalcone OMTs. We calculated differential expression for the core pathway and candidate genes between initial sampling (D_0) and after 4 d (D_4) and 10 d (D_{10}) of bud induction in a growth chamber (Table 1). We calculated $\log_2$-fold changes in expression, and focused on those genes showing $\log_2$-fold changes of >2 in the pairwise comparisons. Using this threshold, we found that *PAL3* expression increased in the leaf buds of both species after 4 d of incubation in the growth chamber. *CHS2*, *CHS3*, and *CHS5* expression showed an increase in *P. trichocarpa*, but in *P. balsamifera* only *CHS1* showed a significant increase (q<0.05). Two candidate OMTs, Potri.013G136300 and Potri.013G143800, had a significant increase in their expression, mirroring the expression pattern displayed by the *PAL* and *CHS* reference genes. Of the *PAL* and *CHS* genes, only *PAL3* in *P. trichocarpa* showed increased expression after 10 d of bud flush. By contrast, Potri.013G136300 and Potri.013G143800 were still highly expressed after 10 d.

Based on phylogenetic and expression analysis, we designated Potri.013G136300 as the primary candidate for OMTs associated with leaf bud resin dihydrochalcones. We also selected two additional candidate genes expressed in both species for further biochemical characterization. Potri.019G102900 was chosen based on its grouping within the same clade as Potri.013G136300 in our phylogeny. Alignment of Potri.019G102900 and Potri.013G136300 revealed 66.86% peptide sequence identity. Potri.013G122400 was selected for further analysis based on its expression pattern matching that of Potri.013G136300 and Potri.013G143800. However, it is more distant in the phylogenetic analysis from the other candidate genes, and more closely related to ObEOMT1 and ObVCOMT1 (Gang *et al.*, 2002). Both of these OMTs methylate eugenols, which are non-flavonoid phenylpropanoid compounds. Potri.013G122400 and Potri.013G136300 share 34.75% sequence identity.

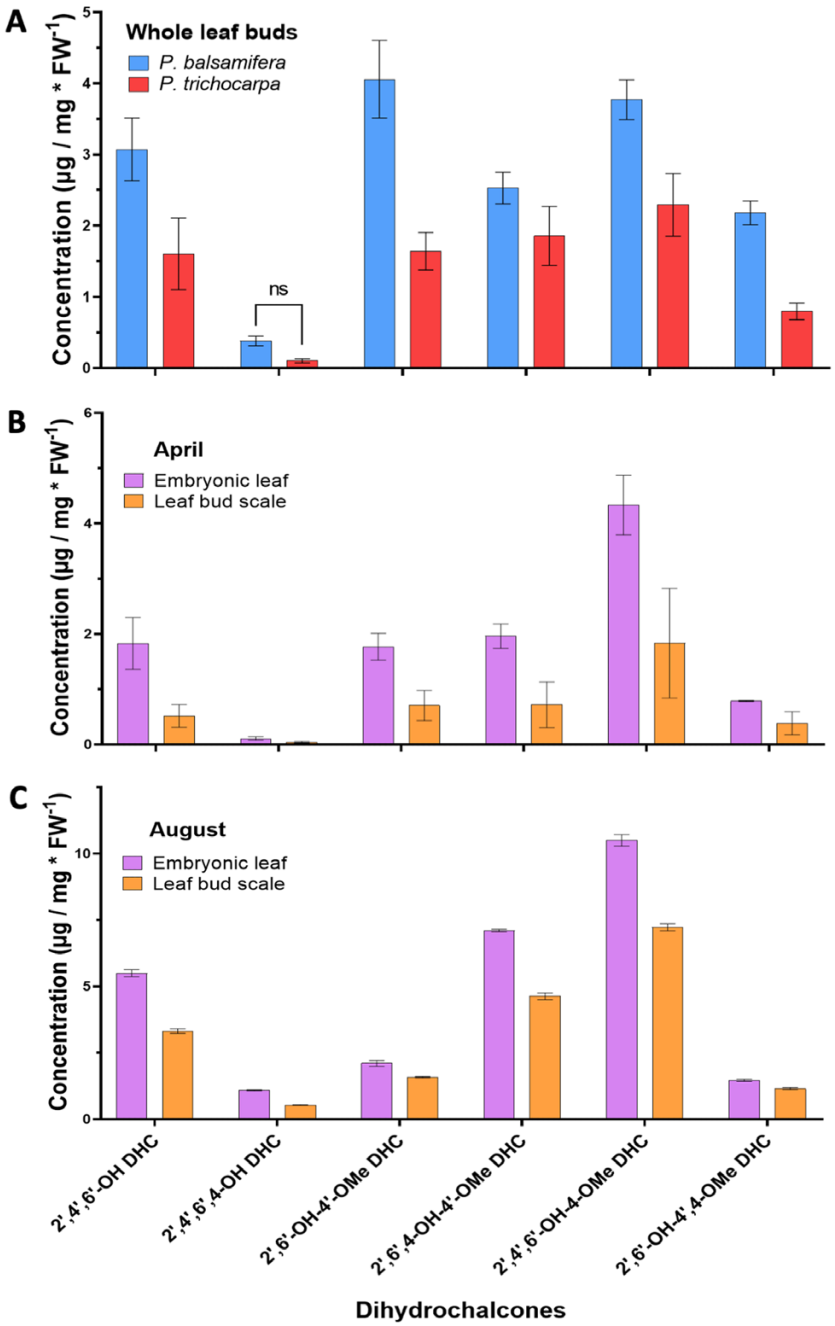

Fig. 2. Analysis of dihydrochalcones in *P. trichocarpa* and *P. balsamifera* lateral leaf buds. Dihydrochalcones in methanolic extracts of *P. trichocarpa* and *P. balsamifera* were quantified by UPLC-MS, and concentrations are expressed per tissue fresh weight. Whole leaf buds of *P. trichocarpa* and *P. balsamifera* were compared (A). *P. trichocarpa* leaf bud scales and embryonic leaf tissue were analyzed separately for April (B) and August (C) samples. Statistical analyses were done by multiple *t*-tests ($P<0.05$), and means ±SD ($n=3$) are shown. All pairwise comparisons [*P. trichocarpa* versus *P. balsamifera* (A), and leaf versus bud samples (B and C)] are significantly different ($P<0.05$) unless indicated as ns (non-significant). Abbreviations are as follows: 2′,4′,6′-OH DHC (2′,4′,6′-trihydroxydihydrochalcone), 2′,4′,6′,4-OH DHC (phloretin), 2′,6′-OH-4′-OMe DHC (2′,6′-dihydroxy-4′-methoxydihydrochalcone), 2′,6′,4-OH-4′-OMe DHC (asebogenin), 2′,4′,6′-OH-4-OMe DHC (2′,4′,6′-trihydroxy-4-methoxydihydrochalcone), and 2′,6′-OH-4,4′-OMe DHC (2′,6′-dihydroxy-4,4′-dimethoxydihydrochalcone).

Biochemical characterization of candidate OMTs

To analyze the biochemical characteristics of the candidate genes, we expressed recombinant N-terminally His-tagged Potri.013G136300, Potri.019G102900, and Potri.013G122400 in *E. coli*. The recombinant proteins were purified by affinity chromatography using an Ni–NTA column. SDS–PAGE

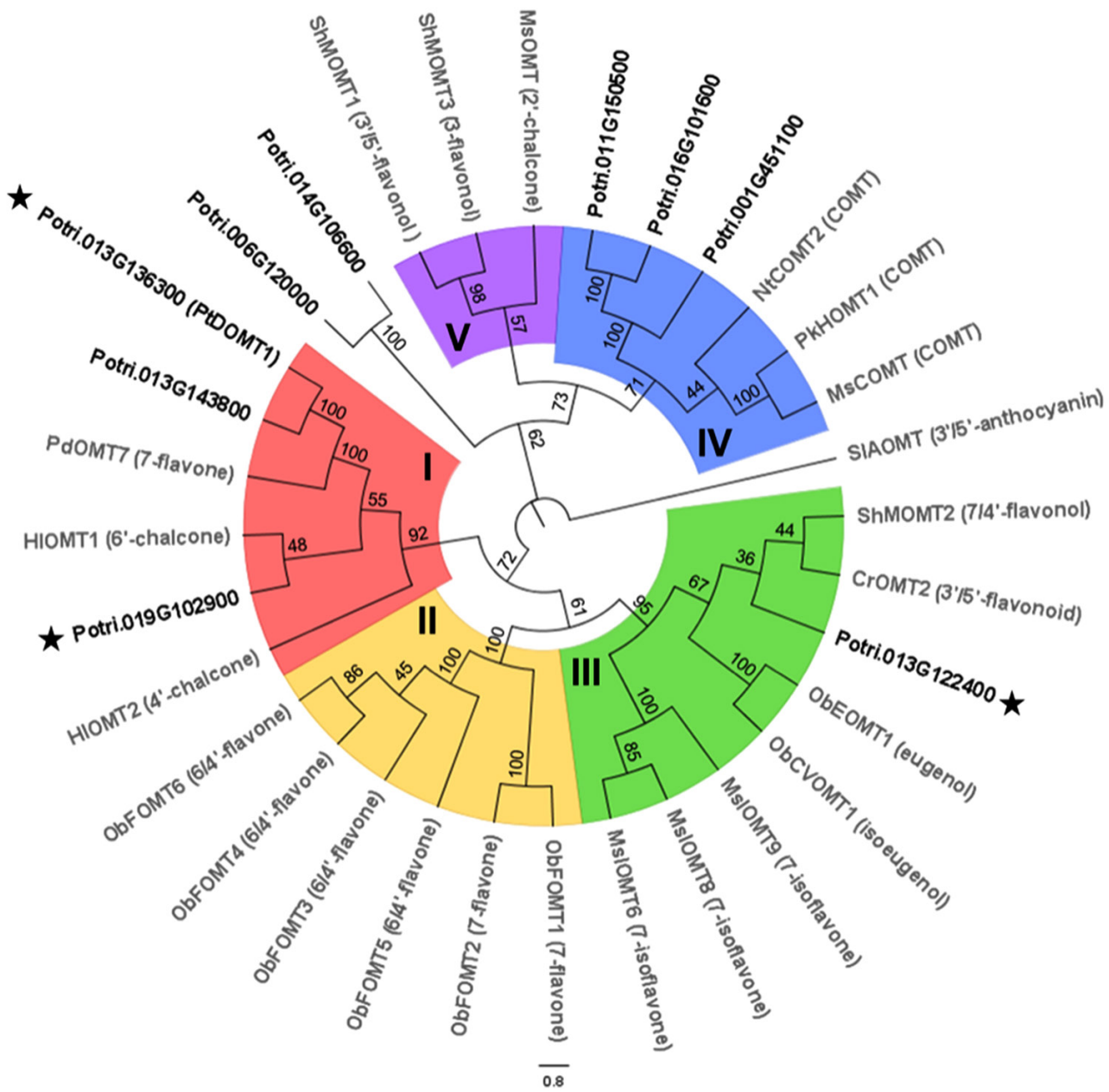

Fig. 3. Phylogenetic analysis of *O*-methyltransferases expressed in *P. trichocarpa* and *P. balsamifera* lateral leaf buds. Maximum-likelihood phylogenetic tree of poplar *O*-methyltransferases expressed in both *P. trichocarpa* and *P. balsamifera* leaf buds. Poplar genes are indicated in black, and other functionally characterized *O*-methyltransferases are indicated in gray. Bootstrap support (1000) is shown as a percentage for each branch. Characterized enzymes have been annotated with their substrate specificity and possible regioselectivity. COMT, caffeic acid 3-*O*-methyltransferase. The stars indicate poplar sequences selected for functional analysis. Five distinct clades are labeled and indicated by color coding.

analysis of the purified product with Coomassie staining and western blot confirmed the expected product sizes (Supplementary Figs S4, S5). The OMT activities of the candidate enzymes were tested using SAM as the methyl donor (Supplementary Fig. S6). Initially, we tested the candidate enzymes using relevant dihydrochalcones as potential substrates. Of the three candidates, only Potri.013G136300 yielded products with any of the tested dihydrochalcone substrate (Fig. 4). Analysis of the reaction products indicated that Potri.013G136300 produced *O*-methylated products with dihydrochalcone aglycones that have unoccupied hydroxyl groups at either 4 (4-OH) or 4′ (4′-OH) positions.The highest relative activity was observed with 2′,4′,6′-OH DHC, which yielded 2′,6′-OH-4′-OMe DHC as the reaction product (Fig. 4B). Assays with the monomethylated 2′,4′,6′-OH-4-OMe DHC or 2′,6′,4-OH-4′-OMe DHC converted either

Table 1. Expression of known phenylpropanoid and flavonoid genes and candidate OMTs based on RNA-seq data of *P. trichocarpa* and *P. balsamifera* lateral leaf buds

		P. trichocarpa				P. balsamifera			
Potri number	**Gene name**	**Log_2 FC (D_4/D_0)[a]**	***q*-value**	**Log_2 FC (D_{10}/D_0)**	***q*-value**	**Log_2 FC (D_4/D_0)**	***q*-value**	**Log_2 FC (D_{10}/D_0)**	***q*-value**
General phenylpropanoid and flavonoid reference genes									
Potri.006G126800	PAL1	1.55	0.000	1.34	0.000	1.28	0.077	–0.45	0.610
Potri.016G091100	PAL3	2.08	0.000	2.51	0.000	2.28	0.010	–0.82	0.440
Potri.014G145100	CHS1	1.29	0.730	–0.29	0.160	2.68	0.002	–0.49	0.670
Potri.001G051500	CHS2	2.49	0.910	0.19	0.150	–	–	–	–
Potri.001G051600	CHS3	2.72	0.330	1.46	0.140	0.30	0.800	–1.39	0.170
Potri.003G176900	CHS5	3.70	0.061	1.48	0.000	0.69	0.430	–1.73	0.033
Candidate *O*-methyltransferases									
Potri.006G120000		–0.12	0.880	0.10	0.780	–0.26	0.380	–0.36	0.210
Potri.001G451100		–1.37	0.062	–3.55	0.000	–0.69	0.400	–0.27	0.790
Potri.011G150500		0.59	0.760	1.35	0.100	–2.29	0.009	–1.11	0.270
Potri.013G122400		**4.27**	**0.000**	**5.46**	**0.000**	**2.23**	**0.000**	**0.36**	**0.350**
Potri.013G136300	**PtDOMT1**	**8.46**	**0.000**	**4.81**	**0.016**	**6.91**	**0.000**	**0.11**	**0.970**
Potri.013G143800		7.09	0.001	3.97	0.063	6.69	0.000	–2.16	0.380
Potri.014G106600		–0.86	0.380	–3.21	0.000	0.75	0.420	2.00	0.020
Potri.016G101600		–0.76	0.720	–4.37	0.080	–2.15	0.021	–0.79	0.470
Potri.019G102900		**0.52**	**0.910**	**1.32**	**0.380**	**–1.43**	**0.220**	**0.88**	**0.520**

[a] Values show log_2 fold change (FC) between the initial sampling (D_0) and samples collected after 4 d (D_4) and 10 d (D_{10}) of bud flush induction. Positive fold change (>2, red) indicates an increase in expression levels, and negative fold change (< –2, blue) a reduction in expression. The *q*-values were calculated from *P*-values adjusted for false discovery rates. Genes highlighted in bold were selected for protein expression and biochemical characterization. Potri.013G136300 was designated PtDOMT1 based on subsequent biochemical analysis.

substrate into the dimethylated 2′,6′-OH-4,4′-OMe DHC. Reactions using 2′,4′,6′,4-OH DHC as a substrate yielded two primary *O*-methylated products, 2′,4′,6′-OH-4-OMe DHC and 2′,6′,4-OH-4′-OMe DHC, confirming that both 4 and 4′ positions are *O*-methylated. Furthermore, an additional product was present at lower concentrations and confirmed as the dimethylated 2′,6′-OH-4,4′-OMe DHC (Fig. 4C). Notably, reactions with 2′,6′-OH-4′-OMe and 2′,6′-OH-4,4′-OMe as substrates yielded no additional products, confirming the enzyme's regiospecificity to the 4 and 4′ positions of dihydrochalcones. When we tested additional phenolic substrates including other flavonoids and benzoic acid esters with the Potri.013G136300 enzyme, no significant products were detected (Supplementary Table S3). Based on these results, we concluded that Potri.013G136300 is a dihydrochalcone-specific OMT which exhibits regioselectivity toward two possible sites for the *O*-methylation reaction. Therefore, we designated Potri.013G136300 as *P. trichocarpa* dihydrochalcone OMT 1 (PtDOMT1).

To determine optimal conditions for PtDOMT1 activity and further investigate the biochemical properties of PtDOMT1, additional reaction conditions and parameters were optimized (Supplementary Fig. S7). The optimum temperature range for the enzyme reaction was 30–35 °C, and the highest activity was observed at pH 7.5. We also determined that under our assay conditions, the enzyme reaction was linear for at least 25 min. Based on the above, we determined Michaelis–Menten kinetic parameters of PtDOMT1 at pH 7.5 and 30 °C using 20 min assays (Fig. 5; Supplementary Fig. S8) with all available substrates. 2′,4′,6′-OH DHC had the lowest K_m (25.1 μM) and the highest turnover rate. Kinetic parameters for the two primary reaction products of 2′,4′,6′,4-OH DHC were calculated separately. Of these, the reaction methylating on the 4′ position (producing 2′,6′,4-OH-4′-OMe DHC) had the lower apparent K_m value (31.0 μM) compared with the competing reaction methylating on the 4 position (producing 2′,4′,6′-OH-4-OMe DHC) (64.0 μM). The reactions using 2′,6′,4-OH-4′-OMe DHC and 2′,4′,6′-OH-4-OMe DHC as the reaction substrates showed very similar K_m values.

Expression analysis of PtDOMT1 in *P. trichocarpa* lateral leaf buds

To investigate the seasonal expression of PtDOMT1 in *P. trichocarpa* leaf buds in the field, we harvested lateral leaf buds monthly over 1 year (Fig. 6A) for analysis by RT–qPCR. Buds are dormant during the winter but begin to expand in March. Bud burst occurs in April as new leaves emerge. In May, very small new buds are present in the axils of the newly formed leaves and continue to expand through the summer. *PtDOMT1* transcripts were only observed from June to October. OMT1 expression increased through the summer season and overlapped with bud maturation (June to August), followed by a drastic reduction in September and October as winter hardening begins. We also dissected lateral leaf buds for the April and August time points in order to measure *PtDOMT1* expression separately in bud scales and the enclosed embryonic leaves. Consistent with our data from whole buds, the expression of *PtDOMT1* was higher in the August dissected buds compared with April (Fig. 6B, C). Interestingly, *PtDOMT1* was expressed in both scales and embryonic leaves. *PtDOMT1* expression was significantly higher in the bud scales compared with leaves in the August buds, but there was no significant difference between the tissues in April.

Discussion

Poplar leaf bud resins are known for their chemical complexity and biological activities with importance for both human and bee health (Vardar-Ünlü *et al.*, 2008; Wilson *et al.*, 2017; Dezmirean *et al.*, 2021). While their phytochemical constituents have been surveyed in a number of *Populus* species, the enzymes for bud resin production have not yet been investigated. Our analysis confirmed the abundance of *O*-methylated dihydrochalcones in leaf buds of *P. trichocarpa* and *P. balsamifera*. Employing a functional genomics approach, we then determined the molecular genetic basis of dihydrochalcone *O*-methylation in these species and identified a new enzyme with novel specificity, PtDOMT1. Its strict substrate preference for dihydrochalcones, regiospecificity, and expression pattern strongly suggest that this enzyme is directly involved in the biosynthesis of the *O*-methylated dihydrochalcones in *P. trichocarpa* and *P. balsamifera*. Our work provides the foundation for the further functional characterization of leaf bud resin formation in poplars.

PtDOMT1 is a dihydrochalcone-specific and regioselective OMT enzyme

Our biochemical characterization of PtDOMT1 demonstrated its specificity towards dihydrochalcones, as it showed no activity with other flavonoids, chalcones, or phenolic glycosides. PtDOMT1 was regioselective and capable of methylating at either the 4 or 4′ positions of dihydrochalcones. Methylation of the 2′ and 6′ positions was not observed. In non-competitive reactions, PtDOMT1 showed the greatest activity with 2′,4′,6′-OH DHC and *O*-methylated the available 4′-OH position. Kinetic parameters of the two monomethylated substrates 2′,4′,6′-OH-4-OMe DHC and 2′,4′,6′-OH-4′-OMe DHC are quite similar, suggesting no clear preference for the 4 or 4′ position if one of them is already methylated. By contrast, in a competitive scenario with 2′,4′,6′,4-OH DHC as a substrate where either position is available, the enzyme was more prone to induce *O*-methylation in the 4-OH position (Fig. 5). This matched the pattern in leaf bud resin profile, showing that 2′,4′,6′-OH-4-OMe DHC is more abundant

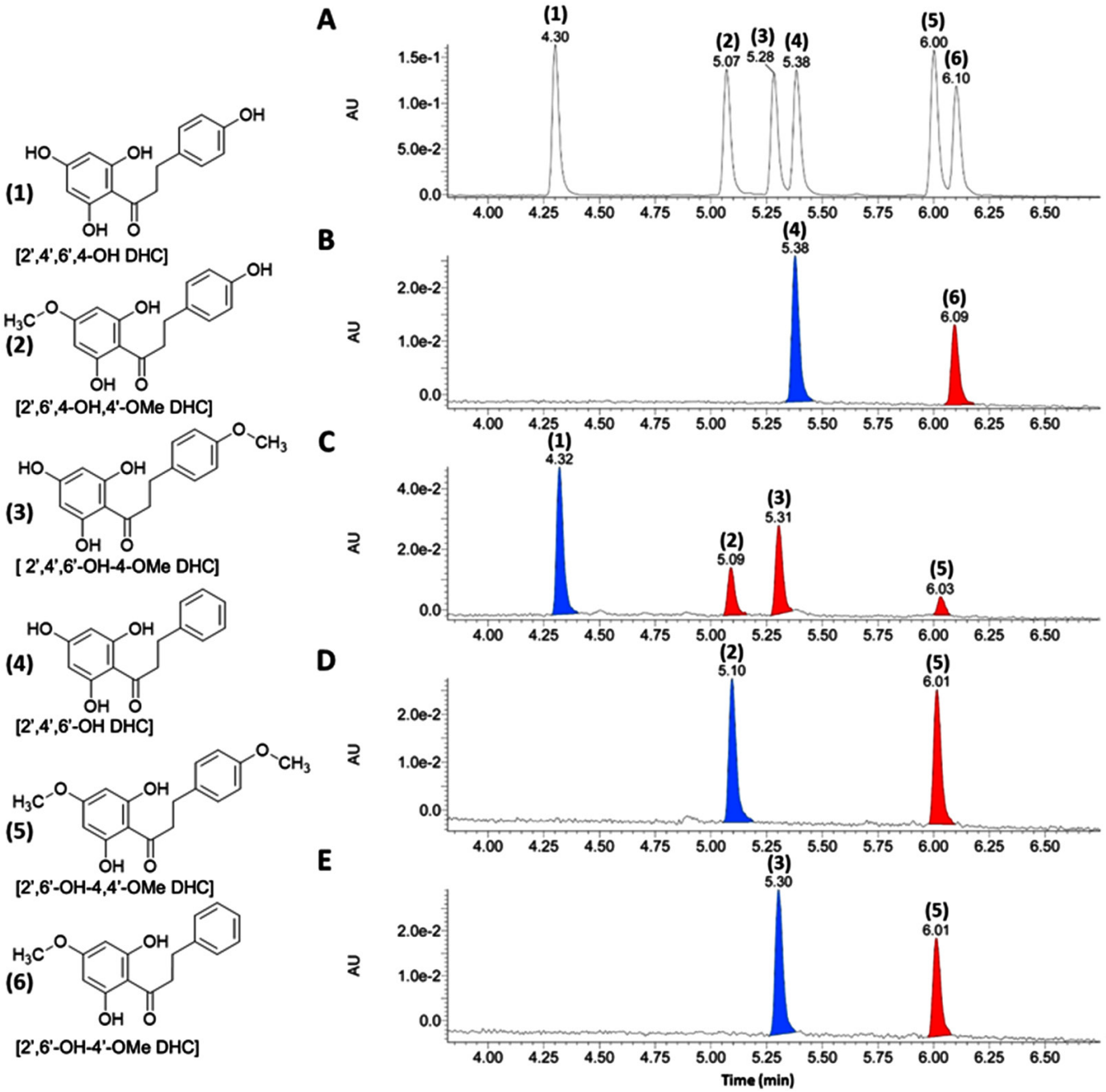

Fig. 4. Enzyme assays of PtDOMT1 with dihydrochalcone substrates. Enzyme assay substrates (blue) and products (red) of PtDOMT1 with dihydrochalcones were analyzed using UPLC-DAD at 280 nm in absorbance units (AU). Peak identities in order of elution are (1) 2′,4′,6′,4-OH DHC (phloretin), (2) 2′,6′,4-OH-4′-OMe DHC (asebogenin), (3) 2′,4′,6′-OH-4-OMe DHC (2′,4′,6′-trihydroxy-4-methoxydihydrochalcone), (4) 2′,4′,6′-OH DHC (2′,4′,6′-trihydroxydihydrochalcone), (5) 2′,6′-OH-4,4′-OMe DHC (2′,6′-dihydroxy-4,4′-dimethoxydihydrochalcone), and (6) 2′,6′-OH-4′-OMe DHC (2′,6′-dihydroxy-4′-methoxydihydrochalcone). Analyzed samples included (A) analytical standard mix containing tested dihydrochalcones, enzyme reaction with (B) 2′,4′,6′-OH DHC, (C) 2′,4′,6′,4-OH DHC, (D) 2′,6′,4-OH-4′-OMe DHC, and (E) 2′,4′,6′-OH-4-OMe DHC.

than 2′,6′,4-OH-4′-OMe DHC in both studied poplar species (Fig. 2). When the enzymatic reaction was extended and left to run for 24 h, both primary products were ultimately *O*-methylated at both the 4 and 4′ positions. These activities provide evidence that PtDOMT1 is involved in the synthesis of the major *O*-methylated dihydrochalcones detected in *P. trichocarpa* and *P. balsamifera*, and thus plays a key role in the biogenesis of leaf bud resin.

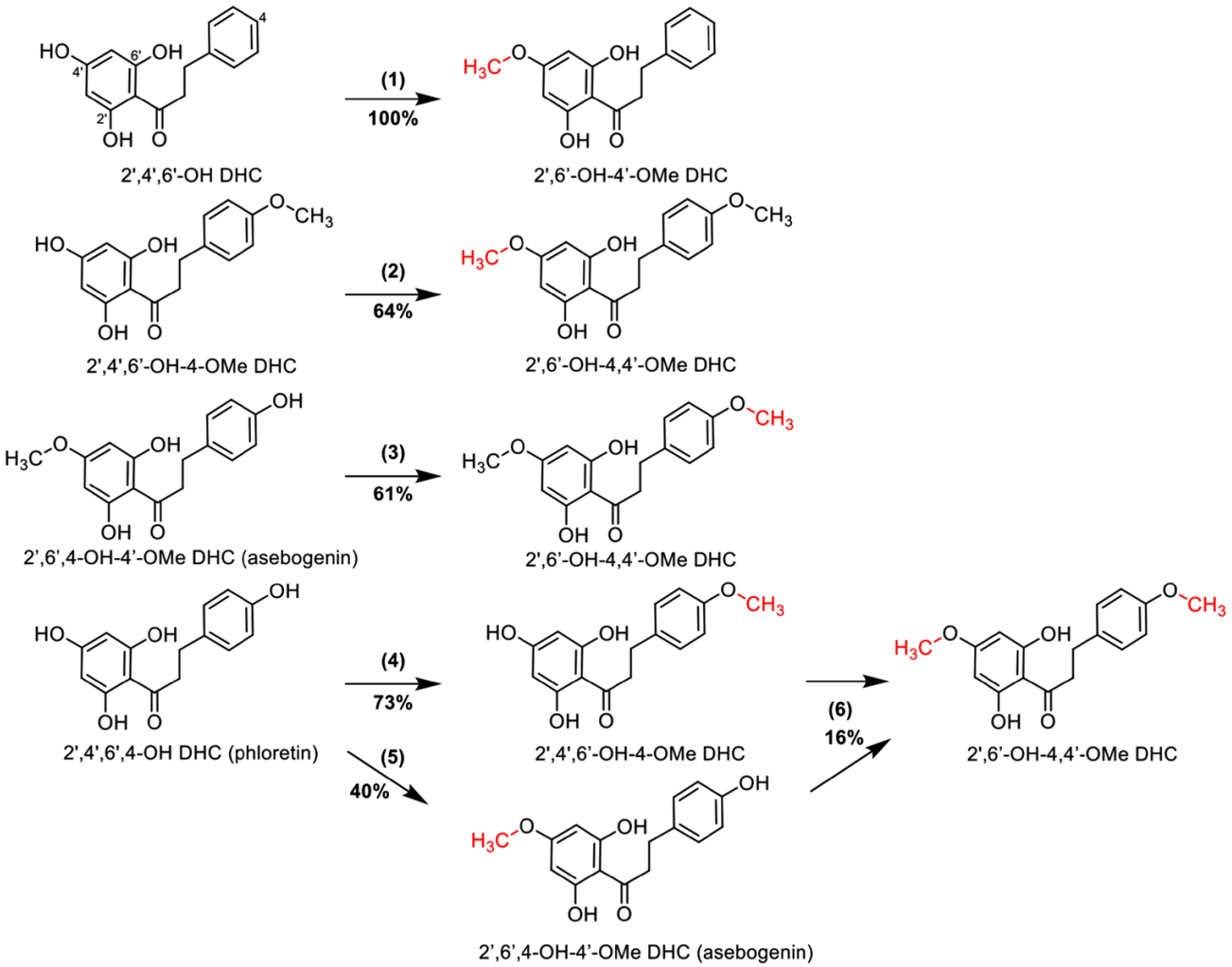

Substrate	Reaction	Product	Relative activity	K_m (μM)	V_{max} (pkat mg^{-1})	V_{max}/K_m
2',4',6'-OH DHC	(1)	2',6'-OH-4'-OMe DHC	100 %	25.1 ± 3.6	11.7 ± 0.8	0.47
2',4',6'-OH-4-OMe DHC	(2)	2',6'-OH-4,4'-OMe DHC	64 %	57.0 ± 5.8	7.6 ± 0.3	0.13
2',6',4-OH-4'-OMe DHC	(3)	2',6'-OH-4,4'-OMe DHC	61 %	59.1 ± 7.0	7.7 ± 0.5	0.13
2',4',6',4-OH DHC	(4)	2',4',6'-OH-4-OMe DHC	73 %	64.0 ± 2.5	9.8 ± 0.4	0.15
	(5)	2',6',4-OH-4'-OMe DHC	40 %	31.0 ± 5.7	5.2 ± 0.3	0.17
	(6)	2',6'-OH-4,4'-OMe DHC	16 %	-	-	-

Fig. 5. Relative activity and Michaelis–Menten kinetic parameters for PtDOMT1 with different dihydrochalcone substrates. The top panel shows reactions carried out by PtDOMT1 and the relative activity under standard conditions. Abbreviations are as in Fig. 2. Reaction with phloretin yielded two primary products: 2′,4′,6′-OH-4-OMe DHC and asebogenin, and a secondary product, 2′,6′-OH-4,4′-OMe DHC. Michaelis–Menten kinetic parameters were computed using non-linear regression analysis based on the concentration of enzyme reaction products under standard conditions, as described in the Materials and methods. Kinetic parameters of phloretin are indicated separately for the two primary products produced competitively in the assays. The data represent the means (±SD) of independent PtDOMT1 recombinant protein preparations (n=3).

While no other plant dihydrochalcone-specific OMTs have been reported, the regiospecificity for 4 and 4′ positions we observed is typical for flavonoid OMTs, which often methylate the 4′ and 7 positions of flavonoids (equivalent to the 4 and 4′ position of dihydrochalcones). Regioselective OMTs with a similar capability to produce two subsequent methoxylations in different positions of aromatic rings of flavonoid structures have been previously reported. In *S. habrochaitis*, ShMOMT2 can methylate the 7 and 4′ positions of flavonols but prefers the former (Schmidt *et al.*, 2011). By contrast, ShMOMT1

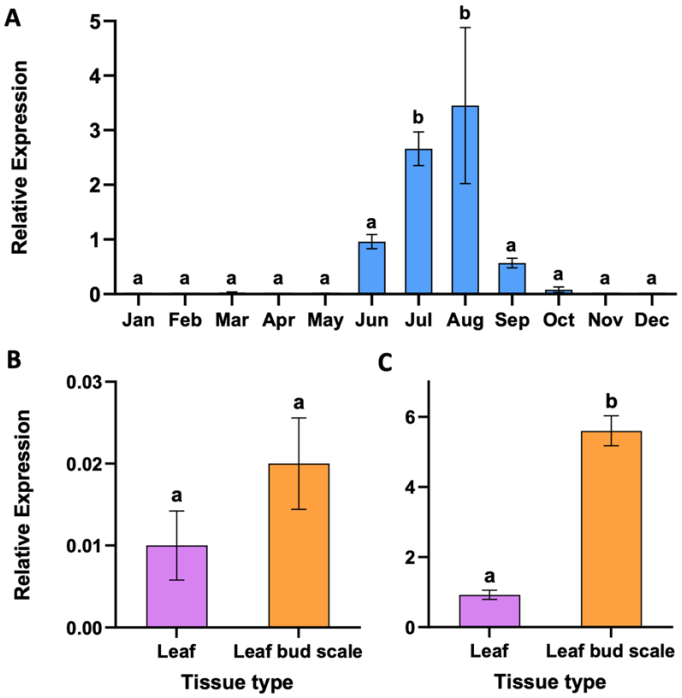

Fig. 6. Expression of *PtDOMT1* in *P. trichocarpa* lateral leaf buds across seasons and different bud tissues. The expression of *PtDOMT1* was analyzed using RT–qPCR, as described in the Materials and methods. The relative expression was measured in (A) whole leaf buds over the annual dormancy–growth cycle. Leaf bud scales and embryonic leaves were collected in (B) April and (C) August. The data represent means ±SD (n=3). Significant differences (P<0.05) between the samples are indicated by different letters as determined by Tukey's HSD.

methylates only 3′ and 5′ positions of quercetin and myricetin. Similarily, in sweet basil (*O. basilicum*), ObFOMT3, ObFOMT4, ObFOMT5, and ObFOMT6 carry out 6- and 4′-*O*-methylations of flavones (Berim *et al.*, 2012). Although these OMTs can act on both positions, they display a higher affinity towards one of them, with subtle different changes in amino acid residues determining this regioselectivity (Berim *et al.*, 2012). Consequently, the relative activity toward the subsequent substrate is reduced after the initial reaction where the preferred position is occupied. PtDOMT1 displayed similar behavior with phloretin (2′,4′,6′,4-OH) as substrate: it preferred the 4 position but subsequently methylated the 4′ position (Fig. 5).

Identification of the amino acid residues involved in defining the regioselectivity of PtDOMT1 could enable the design of enzymes with novel regiospecificity towards dihydrochalcones or other molecules (Jockman *et al.*, 2023). For example, directed mutagenesis of the amino acid residues lining the active site of a bacterial OMT enhanced activity of the enzyme towards dihydrochalcones (Kunzendorf *et al.*, 2023). Enzymes with specificity towards the 4 position of the dihydrochalcones could find application in the synthesis of neohesperidin, an artificial sweetener (Kunzendorf *et al.*, 2023). Furthermore, the sensitivity of single amino acid substitutions for regiospecificity has been demonstrated. A random screening of *P. deltoides* POMT7 mutations based on error-prone PCR found that substituting Gly for Asp at position 257 allowed the recombinant enzyme to methylate at position 3 as well as at position 7 of quercetin and kaempferol (Joe *et al.*, 2010). Interestingly, a preliminary analysis of the PbDOMT1 amino acid sequence which we compiled from the *P. balsamifera* transcriptome data also showed an amino acid difference at Asp257 relative to the PtOMT1 sequence (Supplementary Fig. S9). This could suggest slightly different substrate preference or regiospecificity for the *P. balsamifera* enzyme. A direct comparison of OMT1 from *P. trichocarpa* and *P. balsamifera*, and OMT7 from *P. deltoides* would test how the substrate selectivity and regiospecificity of these enzymes differs in the context of their phenolic profiles.

Although we hypothesized that phylogenetic analysis could group enzymes of similar substrate specificity or regioselectivity, closer inspection suggests that this may not hold consistently for these enzymes. The *P. deltoides* POMT7 clusters closely with PtDOMT1 but accepts flavones and flavonols, and no activity with chalcones or dihydrochalcones was reported (Kim *et al.*, 2006). PtDOMT1 is specific for 4 or 4′ positions and is similar to the HlOMT2 from hop (*H. lupulus*), which preferentially methylates the 4 position of chalcones (Nagel *et al.*, 2008). However, HlOMT2 is active with a much broader ranges of substrates than PtDOMT1. Likewise, the closely related flavone OMT from poplar methylates the 7 position of flavones and flavonols (Kim *et al.*, 2006), which is analogous to the 4′ position of chalcones. By contrast, hop HlOMT1 groups with the same clade as PtDOMT1 but is specific for the 6′ position and leads to the synthesis of xanthohumol (Nagel *et al.*, 2008). Other OMTs with specificity for the 7 position of flavones are found in clades II and III, for example ShMOMT2 from *S. habrochaites* (Fig. 3). Clade V also includes OMTs that can methylate flavonoids in various positions; for example, ShOMT1 and ShOMT3 are able to act on the 3′,5′ position or 3′ position of myricetin, respectively. Therefore, while phylogenetic analysis can help suggest additional OMTs or substrates of relevance for poplar bud resin biosynthesis, direct assays with recombinant enzyme are needed to determine actual substrates and regiospecificity.

Interestingly, PtDOMT1 did not show any significant enzymatic activity with naringenin chalcone (Supplementary Table S3), since the methoxylated versions of this flavonoid (2′,6′,4-trihydroxy-4′-methoxychalcone and 2′,4′,6′-trihydroxy-4-methoxychalcone) are found in minor quantities in *P. trichocarpa* resin (English *et al.*, 1991). Likewise, *O*-methylated flavanones corresponding to pinocembrin and naringenin (5-hydroxy-7-methoxyflavanone and 5,4′-dihydroxy-7-methoxyflavanone) are found in *P. trichocarpa* resin, though in lower concentrations than the *O*-methylated dihydrochalcones (English *et al.*, 1991). These observations imply the presence of additional OMT enzymes in leaf buds specific for these

flavonoid classes. However, the other two candidate OMTs tested here also did not show significant activity with naringenin and pinocembrin or their respective chalcones. A systematic survey of the additional OMTs identified by RNA-seq and found to be expressed in leaf buds here provides a starting point for identifying these chalcone- and flavanone-specific OMTs.

Expression of PtDOMT1 provides insight into the timing and location of resin synthesis

The dormancy–growth cycle in poplar leaf buds is regulated by environmental signals, such as temperature and photoperiod (Rohde *et al.*, 2007; Ruttink *et al.*, 2007; Conde *et al.*, 2017). Analysis of *PtDOMT1* gene expression in *P. trichocarpa* lateral leaf buds collected over a full year showed that *PtDOMT1* was expressed primarily from June to September, with a peak in July and August. While our observations only covered 1 year and growing season, it is reasonable to conclude that resin synthesis occurs primarily during the bud maturation and early dormancy induction phases of lateral bud development. We note that our work focused on lateral buds as these are more numerous and can provide greater replication than terminal buds. Terminal buds are formed later in the summer as primary growth stops; thus bud formation and development times in these buds may be more compressed. Analysis of seasonal resin biosynthesis via gene expression studies has not been reported previously; our work suggests that this process is tightly regulated and closely linked to bud development in the summer months. Metabolite analysis of *P. trichocarpa* bud resin during the year confirms this interpretation: newly formed buds in early summer (May–June) have very low dihydrochalcone content, which then increases steeply until September (Piirtola et al., 2025). Lateral bud maturation in late summer and early autumn is followed by the visible appearance of the resin on the bud surface during the autumn months, where it forms a protective layer for the winter.

In addition, our growth chamber data indicate that *PtDOMT1* and flavonoid gene expression can be induced during bud flush, though to a more modest level (Table 1). A lower level of PtDOMT1 expression was also observed when comparing transcript levels in April and August (Fig. 6B). This pattern is consistent with our observations that during spring bud flush of both species, resin droplets again appear on the bud surface. Thus, while the majority of resin synthesis may occur during the summer, additional resin is synthesized in spring during bud flush.

The tissues responsible for resin biosynthesis within the leaf buds have not yet been examined at a biochemical level. If resin synthesis is proportional to dihydrochalcone content, our data would suggest that resin accumulation is greater on the developing leaves within the buds than on the protective scales (Fig. 2). By contrast, PtDOMT1 transcript levels as measured by RT–qPCR were greater in bud scales, especially in August samples (Fig. 6). This could imply that the bud scales are most active in resin synthesis, but that the resin is secreted into the space within the bud which then covers the embryonic leaves. This model is consistent with a detailed anatomical investigation by Curtis and Lersten (1974). These authors observed that resin synthesis occurs in leaf bud scales, which are modified stipules, concurrent with leaf development during bud break and bud formation in *P. deltoides*. Furthermore, their work identified a ridged cell layer with features of a secretory epidermis on the adaxial side of these bud scales (Curtis and Lersten, 1974).

In summary, our work describes the identification of a novel *O*-methyltransferase in *P. trichocarpa* and *P. balsamifera*. PtDOMT1 is specific and leads to *O*-methylation only at 4-OH and 4′-OH positions of dihydrochalcones, thus producing the *O*-methylated compounds highly characteristic of these two species. Our identification of an enzyme associated with seasonal leaf bud resin formation is the first step in more detailed molecular studies of the cellular processes underlying resin production and opens up novel avenues to understand leaf resin bud biosynthesis and function.

Supplementary data

The following supplementary data are available at *JXB* online.

Fig. S1. Time series of *P. balsamifera* lateral leaf buds.

Fig. S2. UPLC-DAD analysis of *P. trichocarpa* and *P. balsamifera* leaf buds.

Fig. S3. UPLC-MS analysis of *P. trichocarpa* and *P. balsamifera* leaf buds.

Fig. S4. Analysis of purified recombinant proteins.

Fig. S5. Analysis of the purified recombinant PtDOMT1.

Fig. S6. The general reaction of *S*-adenosyl-L-methionine with a dihydrochalcone substrate.

Fig. S7. Determination of optimal enzyme reaction conditions for PtDOMT1.

Fig. S8. Kinetic curves of PtDOMT1 reaction with dihydrochalcone substrates.

Fig. S9. Comparison of PtOMT1 amino acid sequence from *P. trichocarpa* and *P. balsamifera*.

Table S1. qPCR primer list.

Table S2. *O*-Methyltransferase genes expressed in lateral leaf buds of *P. trichocarpa* and *P. balsamifera*.

Table S3. Relative activity of PtDOMT1 with different phenolic substrates.

Acknowledgements

We thank Drs Anna Berim and David Gang for providing *Ocimum basilicum* flavonoid *O*-methyltransferase plasmids and advice with enzyme assays. We also thank Dr Raju Soolanayakanahally and Chris Stefner for providing *P. balsamifera* cuttings, Brad Binges for greenhouse and field compound support, and Dr Ori Granot for help with the UPLC-MS analysis.

Author contributions

E-MP: designed and conducted experiments and drafted the manuscript; DM: prepared RNA-seq libraries and helped with transcriptome analysis; JE: co-designed the enzyme assay experiments and edited the manuscript; CPC: helped conceive and design experiments, contributed to writing and editing the manuscript, and obtained funding.

Conflict of interest

No conflict of interest declared.

Funding

This work was supported by the Natural Sciences and Engineering Research Council of Canada (NSERC) to CPC (RGPIN-2020-06646).

Data availability

The data that support the findings of this study are openly available at NCBI Gene Expression Omnibus under GEO accession number GSE289361.

References

Barakat A, Choi A, Yassin NBM, Park JS, Sun Z, Carlson JE. 2011. Comparative genomics and evolutionary analyses of the *O*-methyltransferase gene family in *Populus*. Gene **479**, 37–46.

Berim A, Gang DR. 2016. Methoxylated flavones: occurrence, importance, biosynthesis. Phytochemistry Reviews **15**, 363–390.

Berim A, Hyatt DC, Gang DR. 2012. A set of regioselective O-methyltransferases gives rise to the complex pattern of methoxylated flavones in sweet basil. Plant Physiology **160**, 1052–1069.

Cabanillas BJ, Le Lamer AC, Castillo D, Arevalo J, Estevez Y, Rojas R, Valadeau C, Bourdy G, Sauvain M, Fabre N. 2012. Dihydrochalcones and benzoic acid derivatives from *Piper dennisii*. Planta Medica **78**, 914–918.

Cheng J, Wei G, Zhou H, Gu C, Vimolmangkang S, Liao L, Han Y. 2014. Unraveling the mechanism underlying the glycosylation and methylation of anthocyanins in peach. Plant Physiology **166**, 1044–1058.

Conde D, Le Gac AL, Perales M, Dervinis C, Kirst M, Maury S, González-Melendi P, Allona I. 2017. Chilling-responsive DEMETER-LIKE DNA demethylase mediates in poplar bud break. Plant, Cell & Environment **40**, 2236–2249.

Cui MY, Lu AR, Li JX, *et al*. 2022. Two types of *O*-methyltransferase are involved in biosynthesis of anticancer methoxylated 4′-deoxyflavones in *Scutellaria baicalensis* Georgi. Plant Biotechnology Journal **20**, 129–142.

Curtis JD, Lersten NR. 1974. Morphology, seasonal variation, and function of resin glands on bud and leaves of *Populus deltoides* (*Salicaceae*). American Journal of Botany **61**, 835–845.

Dezmirean DS, Paşca C, Moise AR, Bobiş O. 2021. Plant sources responsible for the chemical composition and main bioactive properties of poplar-type propolis. Plants **10**, 22–20.

English S, Greenaway W, Whatley FR. 1991. Analysis of phenolics of *Populus trichocarpa* bud exudate by GC-MS. Phytochemistry **30**, 531–533.

English S, Greenaway W, Whatley FR. 1992. Analysis of phenolics in bud exudates of *Populus deltoides*, *P. fremontii*, *P. sargentii* and *P. wislizenii* by GC-MS. Phytochemistry **31**, 1255–1260.

Gang DR, Lavid N, Zubieta C, Chen F, Beuerle T, Lewinsohn E, Noel JP, Pichersky E. 2002. Characterization of phenylpropene *O*-methyltransferases from sweet basil: facile change of substrate specificity and convergent evolution within a plant *O*-methyltransferase family. The Plant Cell **14**, 505–519.

Goodstein DM, Shu S, Howson R, *et al*. 2012. Phytozome: a comparative platform for green plant genomics. Nucleic Acids Research **40**, D1178–D1186.

Greenaway W, English S, Weber EW, Whatley FR. 1989. Series of novel flavanones identified by gas chromatography–mass spectrometry in bud exudate of *Populus fremontii* and *Populus maximowiczii*. Journal of Chromatography **481**, 352–357.

Greenaway W, May J, Scaysbrook T, Hatley FRW. 1992. Compositions of bud and leaf exudates of some *Populus* species compared. Zeitschrift fuer Naturforschung **47**, 329–334.

Greenaway W, Whatley FR. 1990. Resolution of complex mixtures of phenolics in poplar bud exudate by analysis of gas chromatography–mass spectrometry data. Journal of Chromatography A **519**, 145–158.

Ibdah M, Martens S, Gang DR. 2018. Biosynthetic pathway and metabolic engineering of plant dihydrochalcones. Journal of Agricultural and Food Chemistry **66**, 2273–2280.

Ibrahim RK, Bruneau A, Bantignies B. 1998. Plant *O*-methyltransferases: molecular analysis, common signature and classification. Plant Molecular Biology **36**, 1–10.

Ibrahim RK, De Luca V, Khouri H, Latchinian L, Brisson L, Chares PM. 1987. Enzymology and compartmentation of polymethylated flavonol glucosides in *Chrysosplenium americanum*. Phytochemistry **26**, 1237–1245.

Jockmann E, Subrizi F, Mohr MKF, Carter EM, Hebecker PM, Popadic D, Hailes HC, Andexer JN. 2023. Expanding the substrate scope of *N*- and *O*-methyltransferases from plants for chemoselective alkylation. ChemCatChem **15**, e202300930.

Joe EJ, Kim BG, An BC, Chong Y, Ahn JH. 2010. Engineering of flavonoid O-methyltransferase for a novel regioselectivity. Molecules and Cells **30**, 137–141.

Kim BG, Kim H, Hur HG, Lim Y, Ahn JH. 2006. Regioselectivity of 7-*O*-methyltransferase of poplar to flavones. Journal of Biotechnology **126**, 241–247.

Kim D, Paggi JM, Park C, Bennett C, Salzberg SL. 2019. Graph-based genome alignment and genotyping with HISAT2 and HISAT-genotype. Nature Biotechnology **37**, 907–915.

Kim BG, Sung SH, Chong Y, Lim Y, Ahn JH. 2010. Plant flavonoid *O*-methyltransferases: substrate specificity and application. Journal of Plant Biology **53**, 321–329.

Koirala N, Thuan NH, Ghimire GP, Thang DV, Sohng JK. 2016. Methylation of flavonoids: chemical structures, bioactivities, progress and perspectives for biotechnological production. Enzyme and Microbial Technology **86**, 103–116.

Kunzendorf A, Zirpel B, Milke L, Ley JP, Bornscheuer UT. 2023. Engineering an *O*-methyltransferase for the regioselective biosynthesis of hesperetin dihydrochalcone. ChemCatChem **15**, e202300951.

Kuś PM, Okińczyc P, Jakovljević M, Jokić S, Jerković I. 2018. Development of supercritical CO_2 extraction of bioactive phytochemicals from black poplar (*Populus nigra* L.) buds followed by GC-MS and UHPLC-DAD-QqTOF-MS. Journal of Pharmaceutical and Biomedical Analysis **158**, 15–27.

Lam KC, Ibrahim RK, Behdad B, Dayanandan S. 2007. Structure, function, and evolution of plant *O*-methyltransferases. Genome **50**, 1001–1013.

Lashley A, Miller R, Provenzano S, Jarecki SA, Erba P, Salim V. 2023. Functional diversification and structural origins of plant natural product methyltransferases. Molecules **28**, 43.

Lavoie S, Legault J, Simard F, Chiasson E, Pichette A. 2013. New antibacterial dihydrochalcone derivatives from buds of *Populus balsamifera*. Tetrahedron Letters **54**, 1631–1633.

Liu Y, Fernie AR, Tohge T. 2022. Diversification of chemical structures of methoxylated flavonoids and genes encoding flavonoid-*O*-methyltransferases. Plants **11**, 564.

Love MI, Huber W, Anders S. 2014. Moderated estimation of fold change and dispersion for RNA-seq data with DESeq2. Genome Biology **15**, 1–21.

Ma D, Reichelt M, Yoshida K, Gershenzon J, Constabel CP. 2018. Two R2R3-MYB proteins are broad repressors of flavonoid and phenylpropanoid metabolism in poplar. The Plant Journal **96**, 949–965.

Mapunya MB, Hussein AA, Rodriguez B, Lall N. 2011. Tyrosinase activity of *Greyia flanaganii* (Bolus) constituents. Phytomedicine **18**, 1006–1012.

Moerman DE. 1998. Native American ethnobotany. Portland, OR: Timber Press.

Muoki RC, Paul A, Kumari A, Singh K, Kumar S. 2012. An improved protocol for the isolation of RNA from roots of tea (*Camellia sinensis* (L.) *O. Kuntze*). Molecular Biotechnology **52**, 82–88.

Nagel J, Culley LK, Lu Y, Liu E, Matthews PD, Stevens JF, Page JE. 2008. EST analysis of hop glandular trichomes identifies an *O*-methyltransferase that catalyzes the biosynthesis of xanthohumol. The Plant Cell **20**, 186–200.

Orjala J, Wright AD, Behrends H, Folkers G, Sticher O, Roegger H, Rali T. 1994. Cytotoxic and antibacterial dihydrochalcones from *Piper aduncum*. Journal of Natural Products **57**, 18–26.

Piirtola E-M, Overy DP, Constabel CP. 2025. Poplar leaf bud resin metabolomics: seasonal profiling of leaf bud chemistry in *Populus trichocarpa* provides insight into resin biosynthesis. Plant and Cell Physiology doi: 10.1093/pcp/pcae149.

Rivière C. 2016. Dihydrochalcones: occurrence in the plant kingdom, chemistry and biological activities. In: Atta-ur-Rahman, ed. Studies in natural products chemistry, Volume 51. Amsterdam: Elsevier, 253–381.

Rohde A, Ruttink T, Hostyn V, Sterck L, Van Driessche K, Boerjan W. 2007. Gene expression during the induction, maintenance, and release of dormancy in apical buds of poplar. Journal of Experimental Botany **58**, 4047–4060.

Ruttink T, Arend M, Morreel K, Storme V, Rombauts S, Fromm J, Bhalerao RP, Boerjan W, Rohde A. 2007. A molecular timetable for apical bud formation and dormancy induction in poplar. The Plant Cell **19**, 2370–2390.

Schmidt A, Li C, Jones AD, Pichersky E. 2012. Characterization of a flavonol 3-O-methyltransferase in the trichomes of the wild tomato species *Solanum habrochaites*. Planta **236**, 839–849.

Schmidt A, Li C, Shi F, Jones AD, Pichersky E. 2011. Polymethylated myricetin in trichomes of the wild tomato species *Solanum habrochaites* and characterization of trichome-specific 3′/5′- and 7/4′-myricetin *O*-methyltransferases. Plant Physiology **155**, 1999–2009.

Szliszka E, Czuba ZP, Mazur B, Paradysz A, Krol W. 2010. Chalcones and dihydrochalcones augment TRAIL-mediated apoptosis in prostate cancer cells. Molecules **15**, 5336–5353.

Trapnell C, Roberts A, Goff L, Pertea G, Kim D, Kelley DR, Pimentel H, Salzberg S, Rinn J, Pachter L. 2012. Differential gene and transcript expression analysis of RNA-seq experiments with TopHat and Cufflinks. Nature Protocols **7**, 562–578.

Vanholme R, Demedts B, Morreel K, Ralph J, Boerjan W. 2010. Lignin biosynthesis and structure. Plant Physiology **153**, 895–905.

Vardar-Ünlü G, Silici S, Ünlü M. 2008. Composition and in vitro antimicrobial activity of *Populus* buds and poplar-type propolis. World Journal of Microbiology and Biotechnology **24**, 1011–1017.

Wilson MB, Pawlus AD, Brinkman D, Gardner G, Hegeman AD, Spivak M, Cohen JD. 2017. 3-Acyl dihydroflavonols from poplar resins collected by honey bees are active against the bee pathogens *Paenibacillus larvae* and *Ascosphaera apis*. Phytochemistry **138**, 83–92.

Wollenweber E, Dietz VH. 1981. Occurrence and distribution of free flavonoid aglycones in plants. Phytochemistry **20**, 869–932.